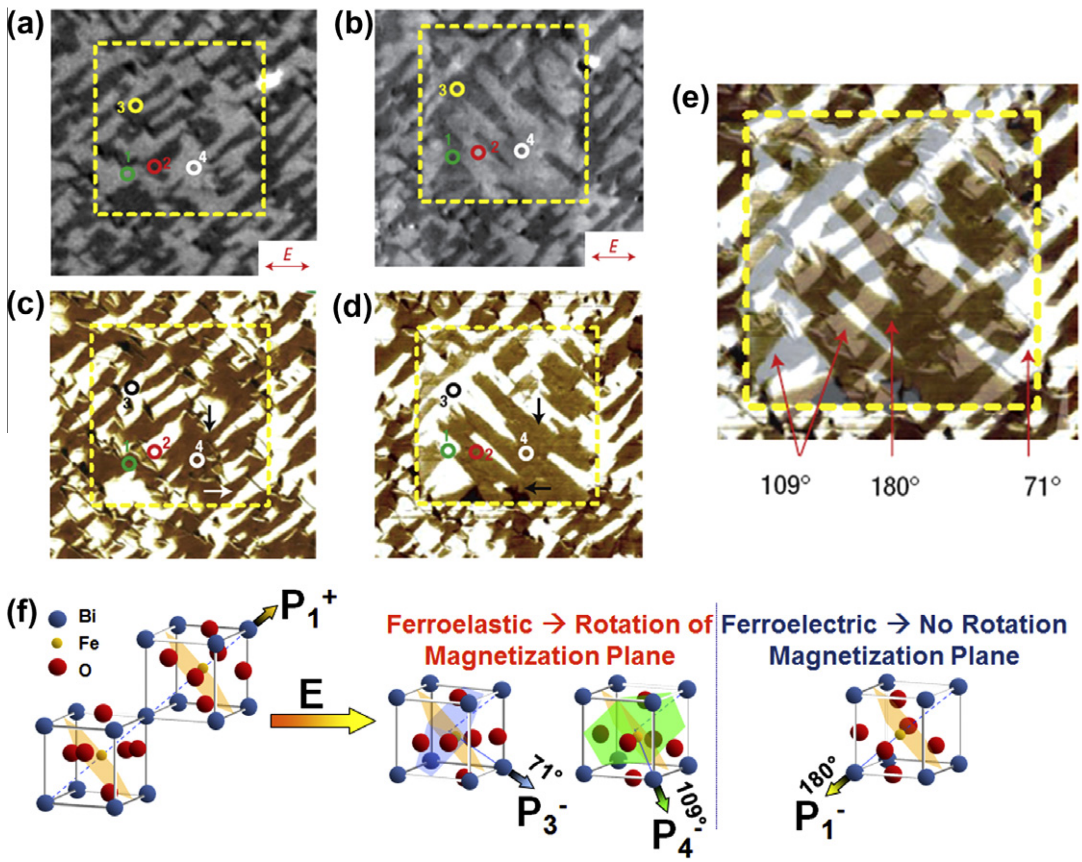

Fig. 6. Determination of strong magnetoelectric coupling in $BiFeO_3$. Photemission electron microscopy (PEEM) images before (a) and after (b) electric field poling. The arrows show the X-ray polarization direction during the measurements. In-plane PFM images before (c) and after (d) electric field poling. The arrows show the direction of the in-plane component of ferroelectric polarization. Regions 1 and 2 (marked with green and red circles, respectively) correspond to 109° ferroelectric switching, whereas 3 (black and yellow circles) and 4 (white circles) correspond to 71° and 180° switching, respectively. In regions 1 and 2 the PEEM contrast reverses after electrical poling. (e) A superposition of in-plane PFM scans shown in (c and d) used to identify the different switching mechanisms that appear with different colors and are labeled in the figure (adapted from Ref. [65]). (f) Schematic illustration of coupling between ferroelectricity and antiferromagnetism in $BiFeO_3$. Upon electrically switching $BiFeO_3$ by the appropriate ferroelastic switching events (i.e. 71° and 109° changes in polarization) a corresponding change in the nature of antiferromagnetism is observed (adapted from Ref. [65]). (For interpretation of the references to color in this figure legend, the reader is referred to the web version of this article.)

MnO_3 [73], $La_{0.7}Ca_{0.3}MnO_3$ [73], and others. These experiments showed great promise and magnetoelectric voltage coefficients up to $\Delta E/\Delta H = 4680$ mV cm^{-1} Oe^{-1} have been observed. Work also continued investigating thin-film heterostructures by combining such ferroelectrics as $Ba_{0.6}Sr_{0.4}TiO_3$, $BaTiO_3$ [76], and PMN–PT [77] with ferromagnets such as $Pr_{0.85}Ca_{0.15}MnO_3$ [76] and Tb–Fe/Fe–Co multilayers [77]; however, these attempts were unable to produce magnetoelectric voltage coefficients above a few tens of mV cm^{-1} Oe^{-1}. Current theories suggest that the in-plane magnetoelectric interface is limiting the magnitude of this coefficient due to the clamping effect of the substrate on the ferroelectric phase [78]. Since the amount of strain that can be imparted by the ferroelectric phase is limited via this in-plane interfacial geometry, the magnetoelectric voltage coefficient can be reduced by up to a factor of five.

3.6. Vertical nanostructures

A seminal paper by Zheng et al. [79] showed that magnetoelectric materials could also be fabricated in a nanostructured columnar fashion (Fig. 7a). By selecting materials that spontaneously separate due to immiscibility, such as spinel and perovskite phases [67], one can create nanostructured phases made of pillars of one material embedded in a matrix of another. Additionally, the large difference in lattice parameters between these phases leads to the formation of pillars with dimensions on the order of 10 nm, ensuring a high interface-to-volume ratio and strong coupling via strain. In this initial paper, researchers reported structures consisting of $CoFe_2O_4$ pillars embedded in a $BaTiO_3$ matrix. Such structures were shown to exhibit strong magnetoelectric coupling (Fig. 7b) via changes in magnetization occurring at the ferroelectric Curie temperature of the matrix material. These nanostructures, in which the interface is perpendicular to the substrate, remove the effect of substrate clamping and allow for better strain-induced coupling between the two phases. An explosion of research into alternative material systems followed as the design algorithm proved to be widely applicable to many perovskite–spinel systems. Nanostructured composites with combinations of a number of perovskite